

Resolution Enhancement of GPR Data Using Bayesian Filtering Optimized by Machine Learning Algorithms

Alireza HAJIAN (✉ dralirezahajian@gmail.com)

Islamic Azad University Najafabad Branch <https://orcid.org/0000-0002-0931-9339>

Rohollah Kimiaefar

Islamic Azad University Najafabad Branch

Research Letter

Keywords: GPR Data Filtering, Bayesian Filtering, ANFIS, FCM

Posted Date: June 29th, 2020

DOI: <https://doi.org/10.21203/rs.3.rs-38051/v1>

License:  This work is licensed under a Creative Commons Attribution 4.0 International License.

[Read Full License](#)

1 **Resolution Enhancement of GPR Data Using Bayesian Filtering Optimized by**
2 **Machine Learning Algorithms**

3
4 Rohollah Kimiaefar¹ ,Alireza Hajian^{2,*}

5 1,2 Department of Physics, Najafabad Branch, Islamic Azad University, Najafabad, Iran.

6 *Email: dralirezahajian@gmail.com (Corresponding author)

7 **ABSTRACT:**

8 Blurring coherence events is the result of applying many spatial and temporal filtering algorithms
9 when they are applied in order to suppress background random noise. Bayesian Filtering (BF) also
10 suffers from mentioned problem. This paper develops a method for optimizing BF by Adaptive
11 Neuro-Fuzzy Inference System (ANFIS) and Fuzzy C-Mean (FCM) clustering. First the structure
12 of the GPR image is extracted using FCM. The structure and output of the BF for a random part of
13 the data are used to produce output values for training ANFIS and after that, by generalizing the
14 trained network to all data, filtered data would be achieved. The proposed method is applied on
15 synthetic data-sets as well as two real 2-D GPR images gathered in an environmental study project.
16 Performance of the method is evaluated by comparing the results of the proposed method to the
17 output of BF. In synthetic data, the SNR value improved 63 percent more than of BF's output and
18 the visual comparison of the results are suggesting better performance in noise cancellation and
19 resolution enhancement, both in synthetic and real data-sets.

20 **KEYWORDS: *GPR Data Filtering, Bayesian Filtering, ANFIS, FCM.***

22 **1. INTRODUCTION**

23 GPR data are contaminated with random noise like all other kinds of geophysical data and this
24 unwanted part of the raw records, negatively affects all further processing and interpreting steps.
25 Furthermore the resolution of the data, in terms of continuity of events, is inversely proportional to
26 the amount of the background random noise [1].

27 Characteristics of the transmitted signal, geology and the amount of the existing random noise, are
28 the most important parameters that a supervising expert would consider and attenuate random
29 noise by using conventional methods such as, filtering based on Hilbert transform [2], median and
30 Wiener adaptive filtering [3] and methods based on multiresolution transforms [4, 5]. In recent
31 years, methods based on artificial intelligence and soft computing are getting more and more
32 popular in all aspects of geophysical methods [6]. Approaching to semi- and fully- automated
33 methods is one of the main reasons of this commonness [7, ?????????].

34 This paper intends to enhance the resolution of the GPR profile data by attenuating background
35 random noise, utilizing powerful potential of the ANFIS and FCM in model discrimination and the
36 ability of BF in random noise attenuation. The automation of the procedure and the performance of
37 the method, in cases where signal to noise ratio is low, are also in the focus of attention.

38 **2. BAYESIAN FILTERING**

39 Bayes filters are a probabilistic tool for estimating the state of dynamic systems based on the
40 bayesian formula where the state of the system refers to the package of dynamic variables which
41 fully describe the system. The noise in the measurements are considered uncertainly even if the
42 true system state is known. The measurements are not deterministic functions of the state, but are
43 considered as distribution of possible values [50]. The time evolution is modeled dynamically that
44 is perturbed by a certain process noise which is used for modeling the uncertainties in the system

45 dynamics. In most cases, the system is not truly stochastic, but is considered in such way to
 46 represent the model uncertainties.

47 Using a stochastic discrete-time state transition (Eq. 1) and an observation process (Eq. 2), any
 48 nonlinear stochastic system could be defined as [8]:

$$x_n = f_n(x_{n-1}, w_{n-1}) \quad (1)$$

$$y_n = h_n(x_n, v_n) \quad (2)$$

49 For the n-th sample (or time), x_n stands for system state vector that is not usually observable. w_n is
 50 the noise vector, y_n is observation vector and v_n is the observation noise vector. f_n and h_n relate the
 51 prior state to the current state and the current state to the observation vector.

52 The main problem in a typical bayesian context is to measure the posterior density, $p(x_n|y_{1:n})$,
 53 where the set of observations are defined by $y_{1:n} \equiv \{y_1, y_2, \dots, y_n\}$.

54 The mentioned nonlinear and non-Gaussian state-space model (Eq. 1), specifies the predictive
 55 conditional transition density, $p(x_n|x_{n-1}, y_{1:n-1})$, of the current state, considering the previous state
 56 and all previous observations. Also, the observation process equation, Eq. 2, determines the
 57 likelihood function of the current observation given the current state, $p(y_n|x_n)$ [8].

58 The prior probability is defined by Bayes' rule as:

$$p(x_n|y_{1:n-1}) = \int p(x_n|x_{n-1}, y_{1:n-1}) p(x_{n-1}|y_{1:n-1}) dx_{n-1} \quad (3)$$

59 $p(x_{n-1}|y_{1:n-1})$ is the previous posterior density and The correction step generates the posterior
 60 probability density function from:

$$p(x_n|y_{1:n}) = c \times p(y_n|x_n) \times p(x_n|y_{1:n-1}) \quad (4)$$

61 Where c is a normalization constant.

62 The filtering problem is to estimate the first two moments of x_n given $y_{1:n}$. In a recursive manner
 63 and for a general distribution, $p(x)$, this consists of the recursive estimation of the expected value
 64 of any function of x , like $\langle g(x) \rangle_{p(x)}$, using Eq. 3 and Eq. 4 and requires calculation of integrals of the

65 form [8]:

$$\langle g(x) \rangle_{p(x)} = \int g(x) p(x) \quad (5)$$

67
 68 Usually this integral is solved by numerical approximation as the multivariate distribution of these
 69 kinds of integrals cannot be evaluated in closed form.

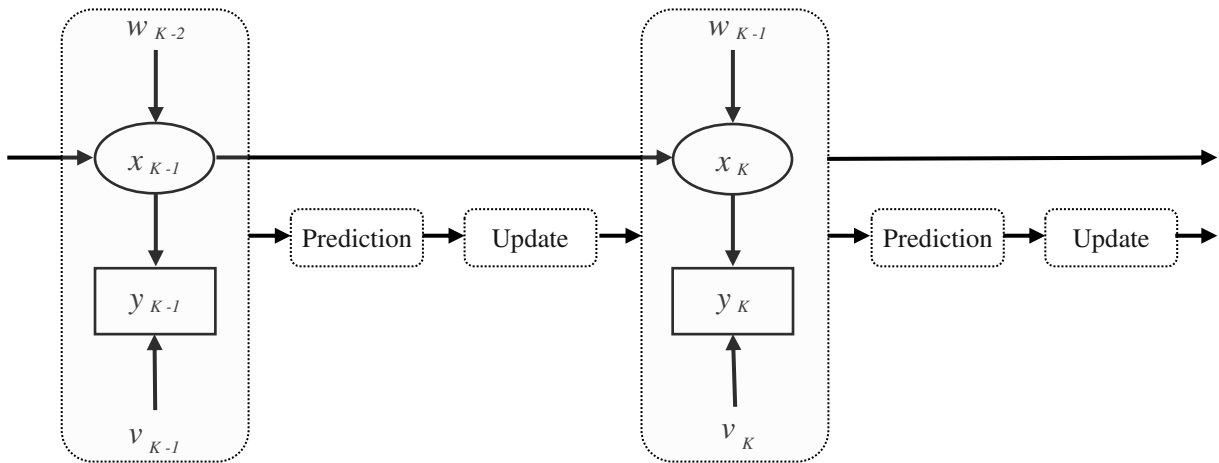


Figure 1: Schematic representation of Bayesian filtering.

70

71

72 **3. METHOD**

73 As illustrated in Fig. 1, in the proposed method, at the very first stage, noise level of the input data
 74 is calculated based on the fact that, higher noise level cause more difference between original

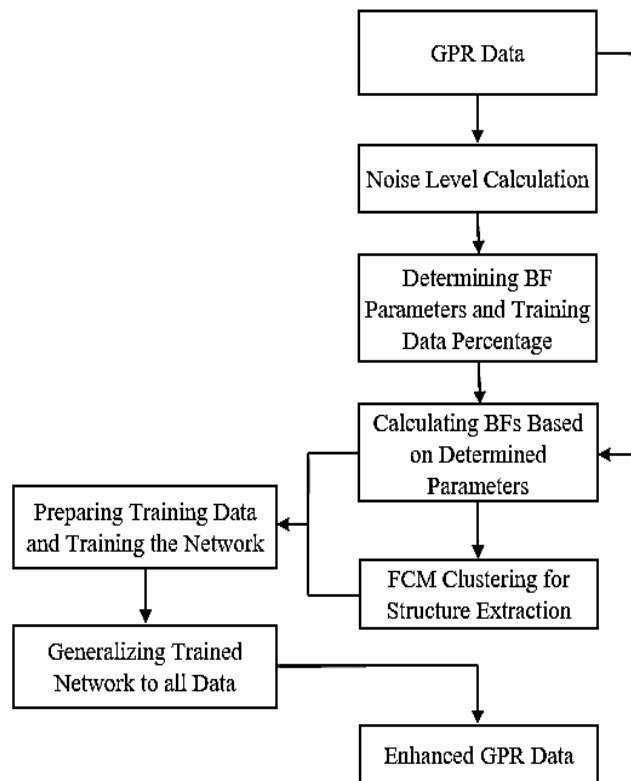


Figure 1: flowchart of the proposed method

75 (noisy) and filtered value and vice versa. Hence computing correlation of the outputs of BFs with
 76 different setups, logically could present an estimation of noise level [10].

77 By comparing known value of the noise variance for a synthetic data (Fig. 4a) with the calculated
 78 noise level, based on mentioned logic in an empirical manner, this method is evaluated and the
 79 result is illustrated in Fig. 2. The calculated noise level has could be considered as the noise
 80 variance with an acceptable approximation. It should be noticed that calculated noise level changes
 81 almost linearly and noise level increase (decrease) could be considered as noise variance increase
 82 (decrease). The calculated noise value has two usage in the method. It is used for determining

83 windows size range (for instance, 3 by 3, to, 17 by 17) and also for determination of training data
84 percentage.

85 At the next step, outputs of BF with different window sizes are calculated. These values are
86 suppliers of FCM clustering input data, for extracting structure of the data, which would be very
87 useful in, especially, denoising data with low signal to noise ratio. Also mentioned values are used
88 for ANFIS training as part of the input data. Among different fuzzy clustering methods, FCM was
89 chosen mainly because of its performance in solving problems in diverse issues [11].

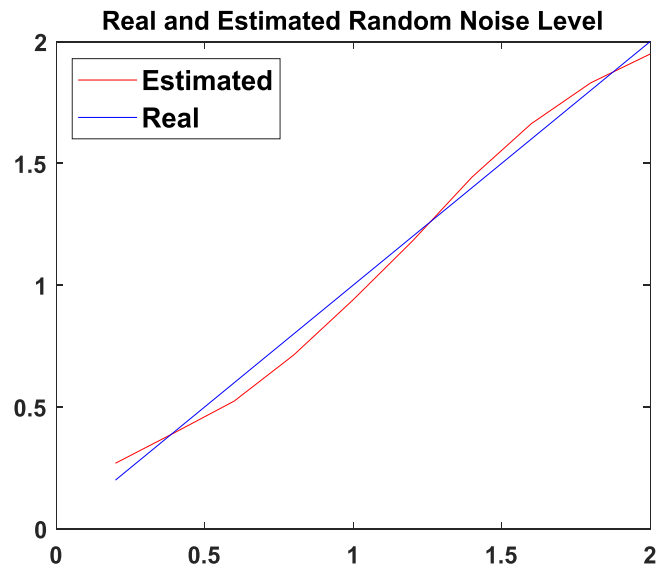


Figure 2: real and calculated noise level for a synthetic 2-D data with different noise variance from 0.2 to 2.

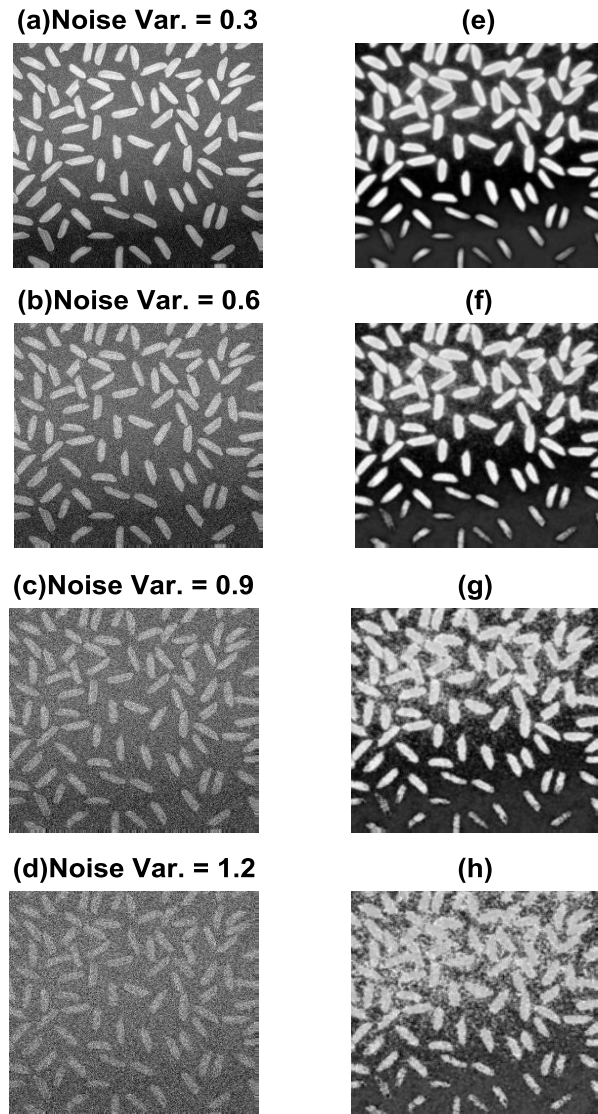


Figure 3: “rice” image with different level of random noise (a to d) and the structure extracted by FCM clustering (g to h respectively).

90 The structure extraction procedure is evaluated by performing the method to the “rice” with
 91 different amount of additive white gaussian random noise. The results of FCM clustering,
 92 structures, are shown in Fig. 3. The noise level is expressed by noise variance here. Although the
 93 clustered data (right column of images is Fig. 3) are showing to have less random components, but
 94 the main reason for calculating them is the ability of providing data structure specially in case data
 95 has high level of additive noise, like Fig. 3c and 3d. In such mentioned circumstances, usually

96 denoising algorithms make the output's details smooth and unattainable. Averaging structure with
97 other components of the output could be an alternative for regular outputs and a way for
98 overcoming the problem.

99 Using original data and the set of BF values for each selected points (as ANFIS input data) and a
100 weighted average of mentioned values as well as extracted structure (as ANFIS output), the
101 training pairs for ANFIS network will be ready. The output of this stage will be automatically
102 achieved by generalizing the trained network to all data. This optimized output or as named here as
103 Bayesian-ANFIS Filtered (BAF) data, will be determined.

104 **4. EXPERMIENTS**

105 The method was tested on one synthetic and two real GPR data-sets which were extracted from a
106 data-set recorded during an environmental study handled by United States Geological Survey
107 (USGS) [12].

108 At the very first step, some zero mean white gaussian noise was added to the synthetic 250 by 250
 109 pixel, layered image. After that, calculating noise level, suggested 10 percent for training data
 110 percentage and a maximum of 17 by 17 window size for BF calculation. A set of 36 inputs
 111 including BF values calculated in 3 to 17 square shape neighborhood, and the value of the pixel (in
 112 noisy data) were contributed in FCM. The number of clusters as mentioned before is two. The
 113 output of FCM provided structure of the data (this structure could be very beneficial in data with
 114 low SNR values). The procedure of filtering proceeded by randomly selecting 10 percent of the
 115 provided data and by weighting the BF values, the output for each row of input data was
 116 determined.

After training data ANFIS network

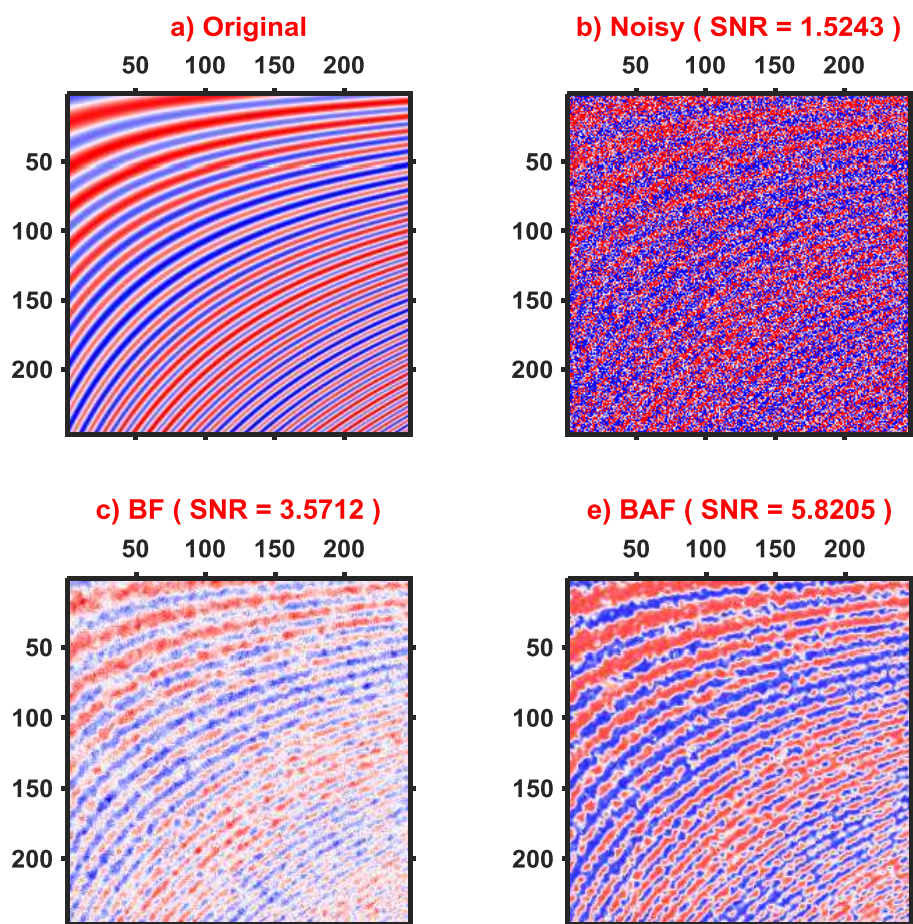


Fig. 4: (a) A synthetic GPR data with varying dips and layer thickness, (b) noisy version (Gaussian random noise added to original image), denoised images by (c) BF and (d) BAF. The output of proposed method is obviously brighter and more interpretable and the SNR has been improved 63 percent more than the output of

117 (Sugeno-type fuzzy inference system), using an initial grid partitioning fuzzy inference system and
118 a hybrid optimization method (least-squares estimation with backpropagation), the trained network
119 was generalized to all data resulting filtered data.

120 The original noise-free synthetic GPR data, noisy version and the data filtered by BF and BAF are
121 illustrated in Fig. 2. The SNR values shown in this figure are calculate by Eq. 6 as:

$$SNR = \frac{P_s}{P_n} \quad (6)$$

122 Where P_s and P_n refer to average power of noise-free data and noise, respectively.

123 Confirmed by SNR values, obviously the performance of BAF is better than BF in eliminating
124 random noise. Note to the high amount of the additive random noise in this data, as the method's
125 ability could be evaluated better in such circumstances.

126 Beside visual and SNR confirmation and as another assessment tool, the cross-section of the
127 original, noisy and filtered images (50th row and column of mentioned data) are plotted in Fig. 4.

128 In terms of performance, efficiency of BAF in recovering the noisy signal could be visually
129 corroborated. In deeper times and far offsets, (Fig. 4a and 4b and samples located between samples
130 150 to 250, where the frequency of layering is relatively higher) original trace has been recovered
131 better by BAF.

132 It should be in the focus of attention that both BF and BAF outputs are structurally same although
133 modified version of BF is more robust in separating noise from original data and resolution
134 enhancement in an adaptive manner.

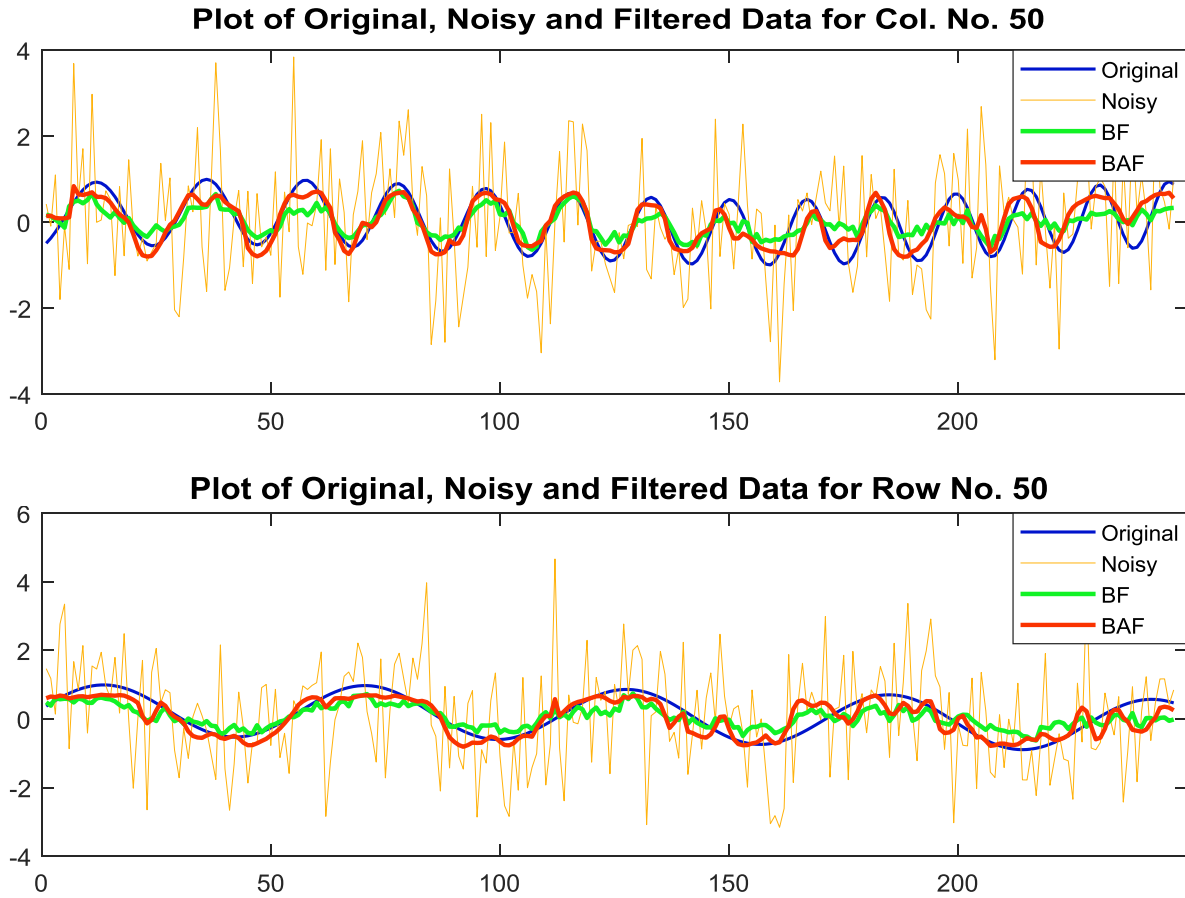


Fig. 5: Cross sections for data plotted in Fig. 4, at column (top) and row (bottom) No. 50. Higher performance could be visually confirmed for the BAF’s output, as its plot is closer to original data plot.

135 As the results from synthetic experiment exhibited the robustness of the proposed method, in the
 136 following, the method is applied to real field data-sets. Illustrated in Fig. 6 and 7, two real GPR
 137 data-sets [12] which are covered with different level of random noise are selected. This first data-
 138 set (Fig. 6) is selected mainly because there are almost two zones with different amplitude
 139 characteristics. The two-phase structure of the data could result in data masking or causing artifacts
 140 on the output. The bottom-left corner of the data which is specified by yellow box, contains some
 141 faulting coherent events. It is expected that an ideal denoising algorithm not to perform much
 142 changes in the structure of this events. For the BF’s output, these events are not clearly showing

143 mentioned faulting system especially in contrast with BAF's output.

144 The second real data-set (Fig. 7) is covered highly with random components. Many of coherent
145 energy is masked and detecting layers could not easily be handled. Having applied BF and BAF

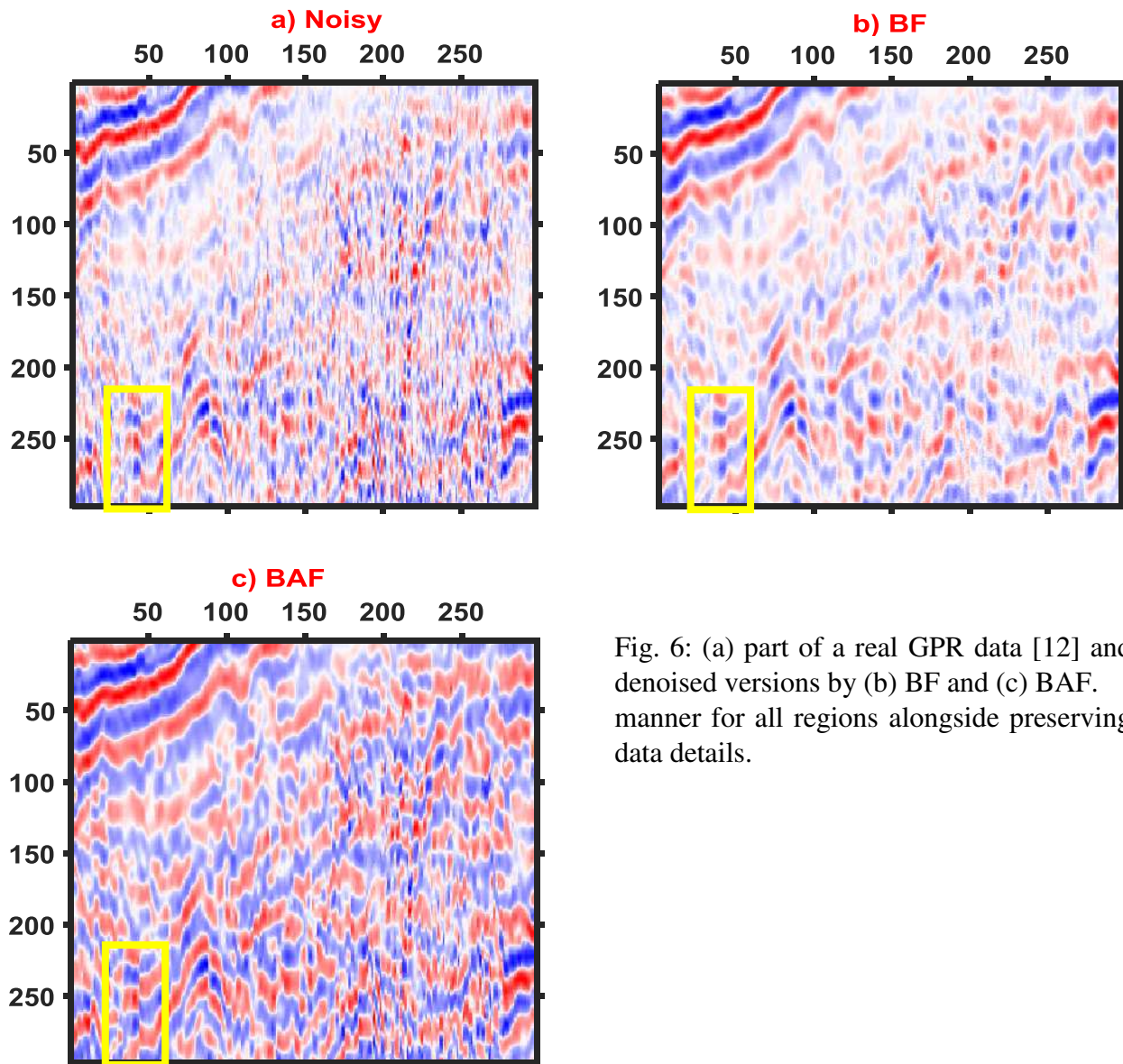


Fig. 6: (a) part of a real GPR data [12] and denoised versions by (b) BF and (c) BAF. manner for all regions alongside preserving data details.

146 (parts b and c in Fig 7) and comparing the resolution of the outputs, confirms the claim that the
147 proposed, ANFIS modified version of BF, can be considered as a powerful alternative for the
148 original BF. In BAF's output, random energy is attenuated strongly in all part of the data in an
149 even manner while the details are preserved in the data.

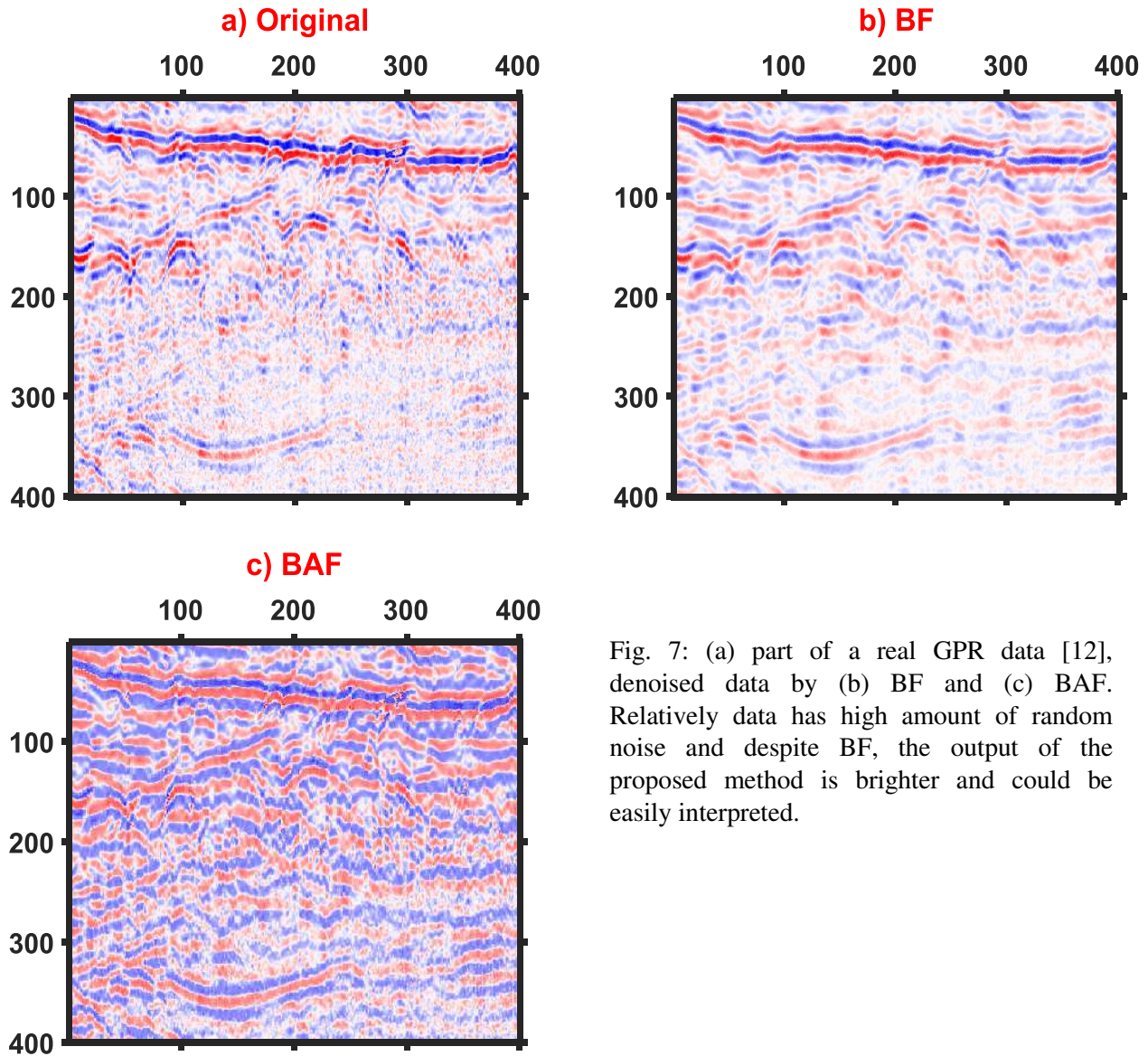


Fig. 7: (a) part of a real GPR data [12], denoised data by (b) BF and (c) BAF. Relatively data has high amount of random noise and despite BF, the output of the proposed method is brighter and could be easily interpreted.

150 **5. CONCLUSIONS**

151 In the method introduced in this paper, the ability of ANFIS and Fuzzy Clustering in model
 152 discrimination and problem solving was used for attenuating random noise in GPR data-sets. BF
 153 calculated with different setups, was used in noise-signal separation, structure extraction and
 154 automation of algorithm. Noise level estimation measure was also used here for determination of
 155 optimized output. The method was applied on one synthetic and two real data-sets and the results

156 showed that BAF has better performance in SNR improvement (more than 2 times) that of BF. In
157 real data-sets, resolution enhanced by proposed method definitely better and event tracing was
158 easier in BAF output.

159 REFERENCES

160 [1] R. E. **Sheriff**, Seismic resolution a key element. **1997**, AAPG Explorer: **18(10)** pp. 44-51.

161 [2] F. **Guangyou**, M. **Pipan**, Synthetic and field examples of ground-penetrating radar (GPR)
162 using two-phase detection techniques. **2003**, *Geophysics*: **68 (2)**: pp. 554–558.

163 [3] Y. **Jeng**, Y. **Li**, C. **Chen**, H. **Chien**, Adaptive filtering of random noise in near-surface seismic
164 and ground-penetrating radar data, **2009**, Journal of Applied Geophysics: **68(1)**, pp. 36-46.

165 [4] Y. **Jeng**, C. **Lin**, Y. **Li**, C. **Chen**, H. **Yu**, Application of sub-image multiresolution analysis of
166 Ground-penetrating radar data in a study of shallow structures, **2011**, Journal of Applied
167 Geophysics, **73(3)**, pp. 251-260.

168 [5] A. **Tzanis**, The Curvelet Transform in the analysis of 2-D GPR data: Signal enhancement and
169 extraction of orientation-and-scale-dependent information, **2015**, Journal of Applied Geophysics:
170 **115**, pp. 145-170.

171 [6] R. **Kimiaefar**, H. **Siahkoochi**, A. **Hajian**, A. **Kalhor**, Seismic random noise attenuation using
172 artificial neural network and wavelet packet analysis, **2016**, Arabian Journal of Geosciences, **9**:
173 234.

174 [7] R. **Kimiaefar**, H. **Siahkoochi**, A. **Hajian**, A. **Kalhor**, Random noise attenuation by Wiener-
175 ANFIS filtering, **2018**, Journal of Applied Geophysics: **159** pp. 453-459.

- 176 [8] A. J. Haug, A Tutorial on Bayesian Estimation and Tracking Techniques Applicable to
177 Nonlinear and Non-Gaussian Processes, 2005, MITRE Technical Report. MTR 05W0000004, The
178 MITRE Corporation.
- 179 [9] X. **Liu**, M. **Tanaka**, M, **Okutomi**, Noise Level Estimation Using Weak Textured Patches of a
180 Single Noisy Image, **2012**, IEEE International Conference on Image Processing.
- 181 [10] R. **Fani**, H. **Hashemi**, Random noise attenuation by application of GK clustering on relevant
182 seismic attributes. **2011**, 124th SEG Conference, Tokyo, Japan.
- 183 [11] R. **Suganya**, R. **Shanthi**, Fuzzy C- Means Algorithm- A Review, **2012**, International Journal
184 of Scientific and Research Publications, **2(11)**: pp. 2250-3153.
- 185 [12] A.S. **Forde**, C.G. **Smith**, B.J. **Reynolds**, 2016, Archive of ground penetrating radar data
186 collected during USGS field activity 13BIM01—Dauphin Island, Alabama, April 2013: U.S.
187 Geological Survey Data Series 982, <http://dx.doi.org/10.3133/ds982>.
- 188 [50] S. **Sarkka**, Bayesian Filtering and Smoothing, **2013**, Cambridge University Press.
189
190

Figures

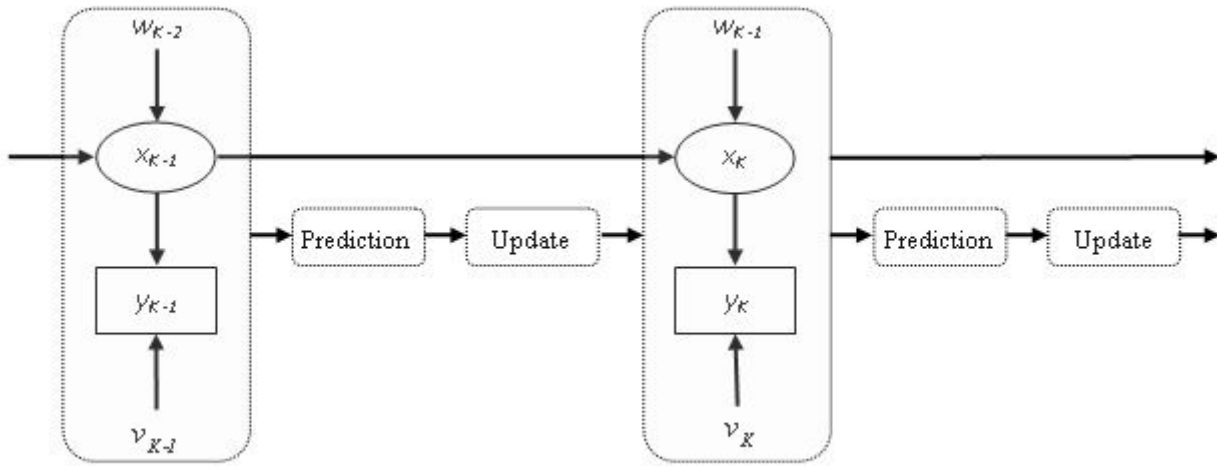


Figure 1 : Schematic representation of Bayesian filtering.

Figure 1

Schematic representation of Bayesian filtering.

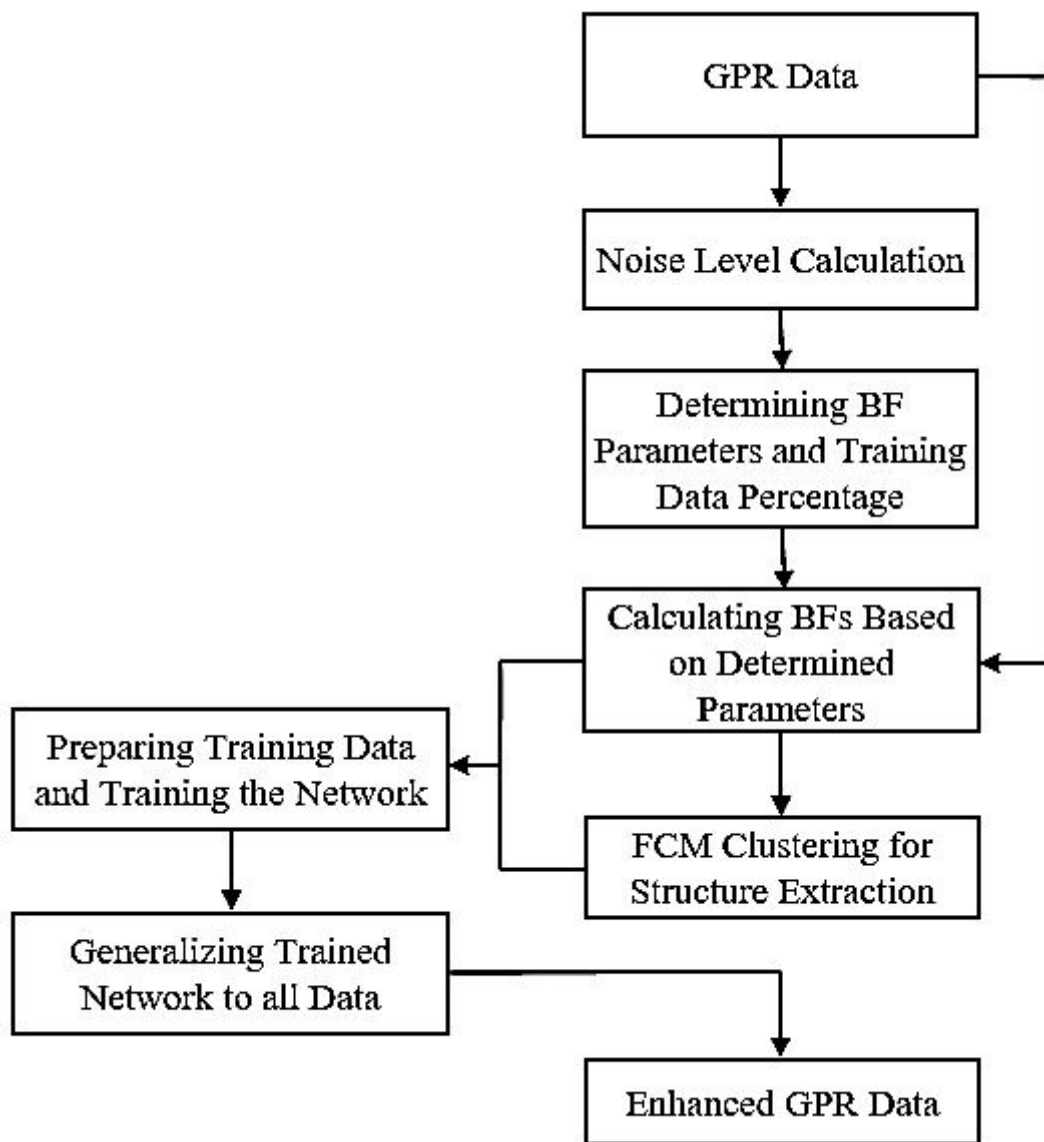


Figure 2

flowchart of the proposed method

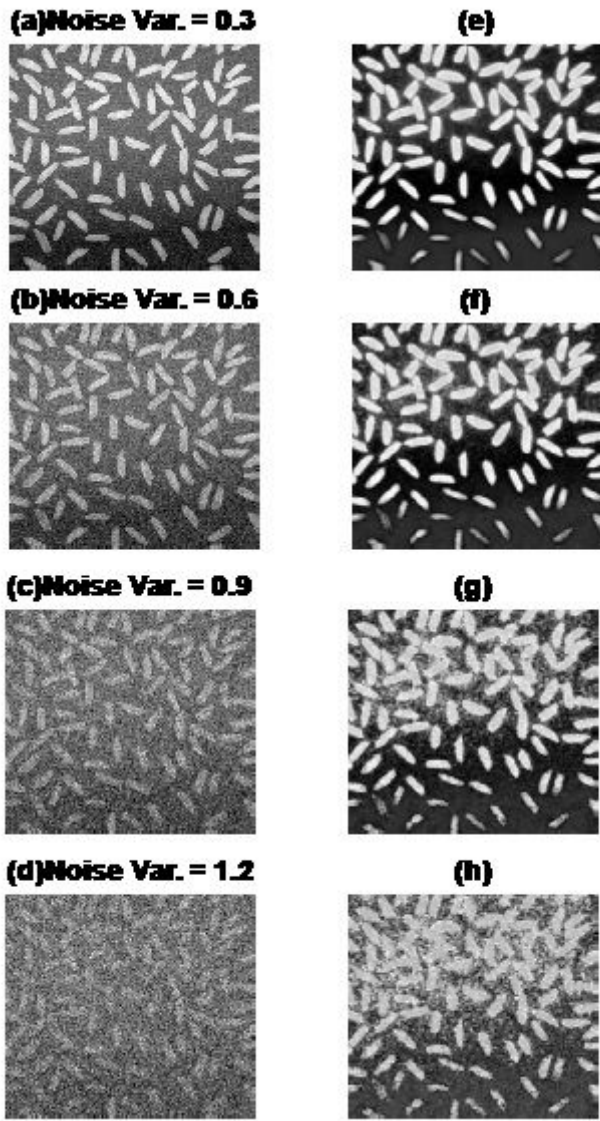


Figure 3

“rice” image with different level of random noise (a to d) and the structure extracted by FCM clustering (g to h respectively).

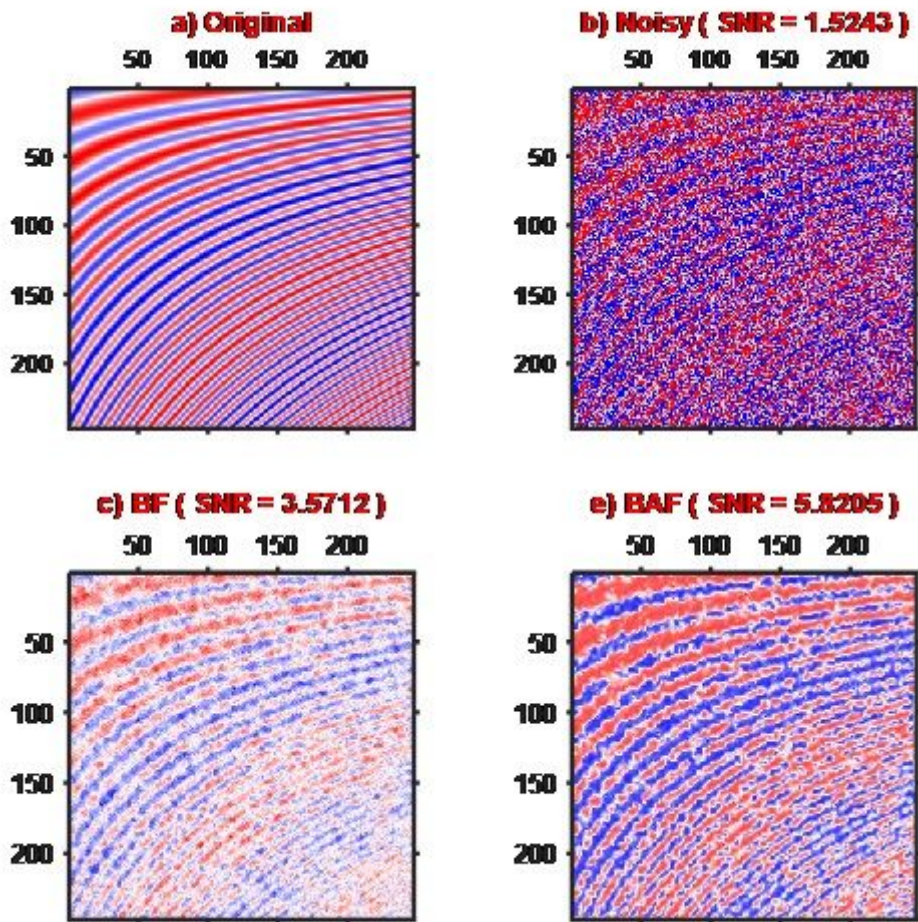


Figure 4

(a) A synthetic GPR data with varying dips and layer thickness, (b) noisy version (Gaussian random noise added to original image), denoised images by (c) BF and (d) BAF. The output of proposed method is obviously brighter and more interpretable and the SNR has been improved 63 percent more than the output of BF.

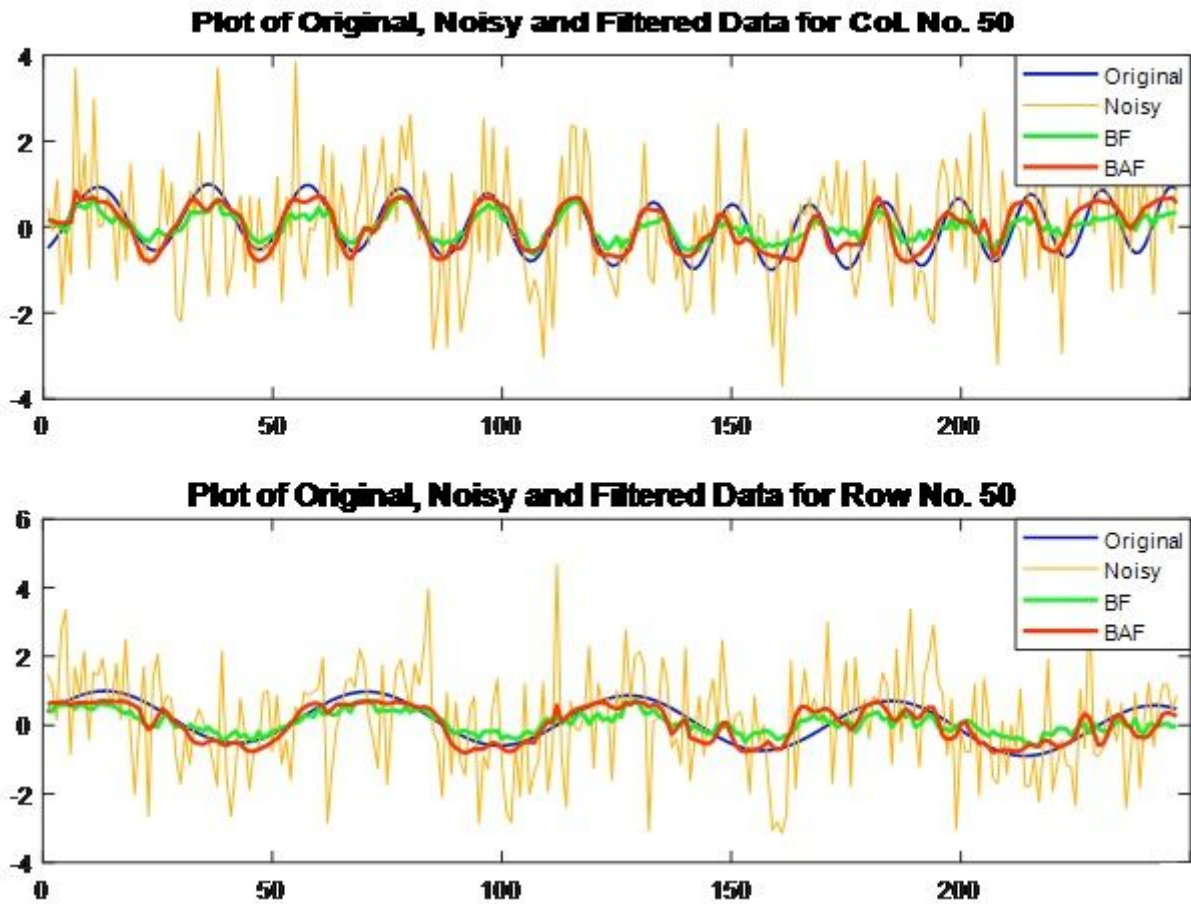


Figure 5

Cross sections for data plotted in Fig. 4, at column (top) and row (bottom) No. 50. Higher performance could be visually confirmed for the BAF's output, as its plot is closer to original data plot.

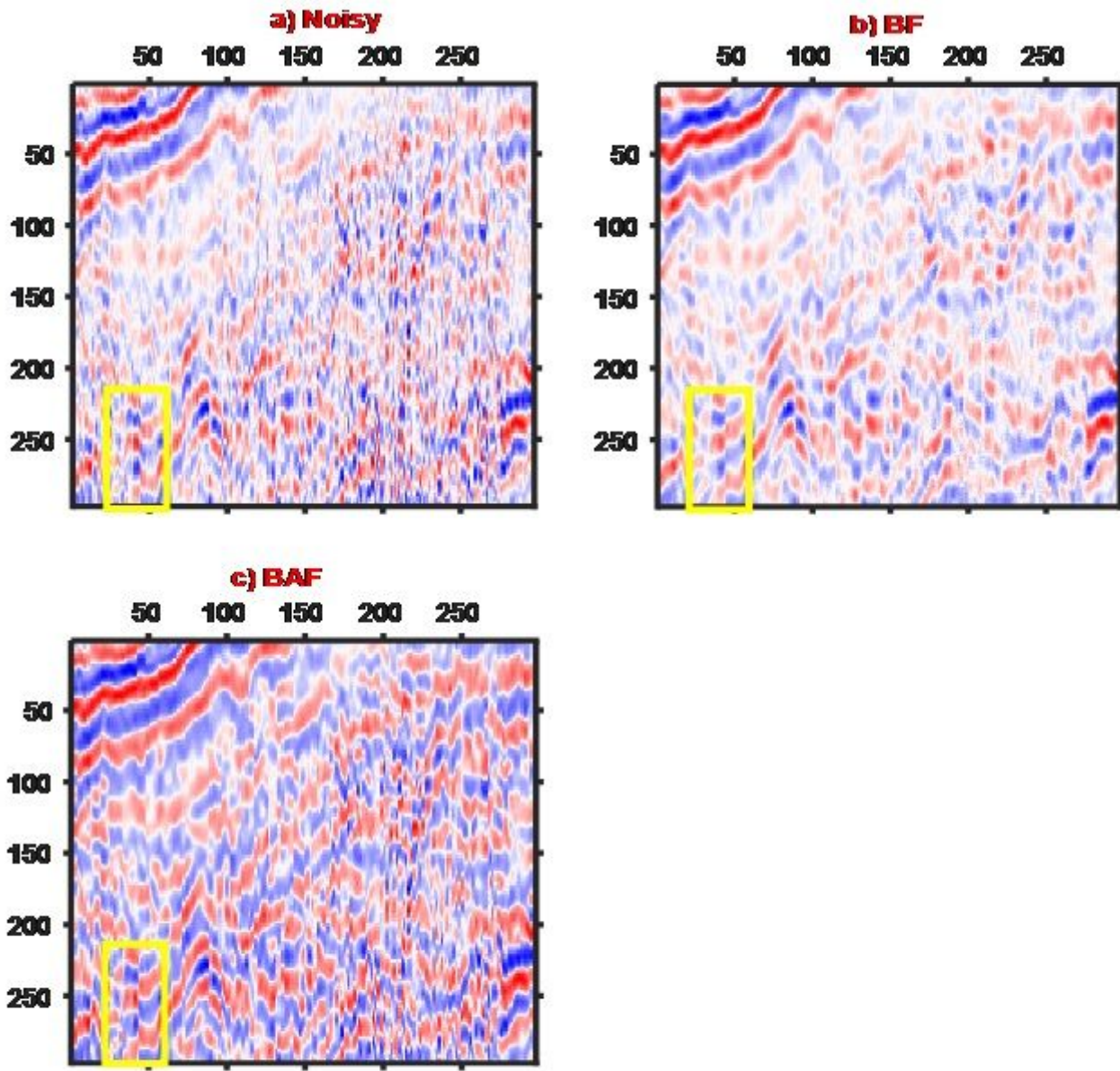


Figure 6

(a) part of a real GPR data [12] and denoised versions by (b) BF and (c) BAF. manner for all regions alongside preserving data details.

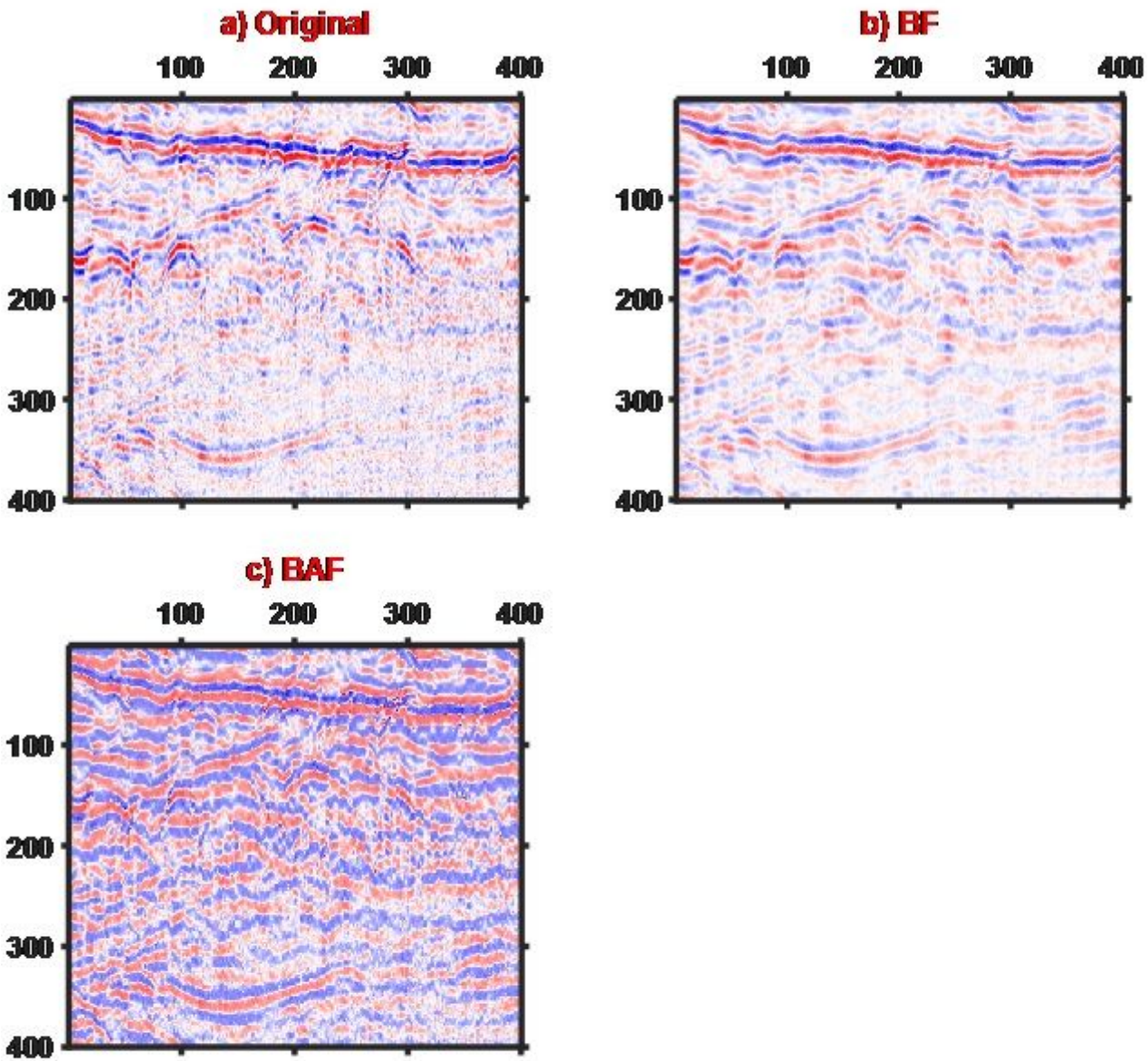


Figure 7

(a) part of a real GPR data [12], denoised data by (b) BF and (c) BAF. Relatively data has high amount of random noise and despite BF, the output of the proposed method is brighter and could be easily interpreted.